LAWRENCE
LIVERMORE
NATIONAL
LABORATORY

UCRL-JRNL-214704

Population of Nuclei Via 7Li-Induced Binary Reactions

R. M. Clark, L. W. Phair, M. Descovich, M. Cromaz, M. A. Deleplanque, P. Fallon, I. Y. Lee, A. O. Macchiavelli, M. A. McMahan, L. G. Moretto, E. Rodriguez-Vieitez, S. Sinha, F. S. Stephens, D. Ward, M. Wiedeking, L. A. Bernstein, J. T. Burke, J. A. Church

August 19, 2005

Physical Review C

Population of Nuclei Via ^{7}Li–Induced Binary Reactions

R.M. Clark, L.W. Phair, M. Descovich, M. Cromaz, M.A. Deleplanque, P. Fallon, I.Y. Lee, A.O. Macchiavelli, M.A. McMahan, L.G. Moretto, E. Rodriguez–Vieitez, S. Sinha, F.S. Stephens, D. Ward, M. Wiedeking

Lawrence Berkeley National Laboratory, Berkeley, California 94720

L.A. Bernstein, J.T. Burke, J.A. Church,

Lawrence Livermore National Laboratory, Livermore, California 94551

(August 18, 2005)

Abstract

We have investigated the population of nuclei formed in binary reactions involving ^{7}Li beams on targets of ^{160}Gd and ^{184}W. The ^{7}Li+^{184}W data were taken in the first experiment using the LIBERACE Ge–array in combination with the STARS Si ΔE–E telescope system at the 88–Inch Cyclotron of the Lawrence Berkeley National Laboratory. By using the Wilczyński binary transfer model, in combination with a standard evaporation model, we are able to reproduce the experimental results. This is a useful method for predicting the population of neutron–rich heavy nuclei formed in binary reactions involving beams of weakly bound nuclei and will be of use in future spectroscopic studies.

PACS numbers: 24.10.-i; 25.70.-z; 25.70.Hi

I. INTRODUCTION

In recent years, there has been increased interest in exploiting massive transfer (also called incomplete fusion) reactions for gamma–ray spectroscopic studies [1–12]. The reason for this interest is that massive transfer reactions offer access to states at relatively high angular momentum in neutron–rich heavy nuclei which are otherwise inaccessible by standard fusion–evaporation reactions involving stable beam–target combinations. Indeed, one may regard such massive transfer reactions as involving 'quasi–radioactive' beams of high intensity. For instance, there is a significant probability of a ^{9}Be beam nucleus breaking up with the emission of a pre–equilibrium α particle while the remaining '^{5}He' fragment fuses with a target nucleus. Similarly, a ^{7}Li nucleus can break up with a triton being captured while an α is emitted.

Massive transfer reactions were recognized and studied many years ago [13–17]. Most of those studies used beams of strongly bound nuclei such as ^{12}C (^{12}C$\rightarrow^{8}$Be+α, S$_{\alpha}$ $\approx$7.4 MeV, S$_{\alpha}$ is the alpha particle separation energy) and ^{16}O (^{16}O$\rightarrow^{12}$C+α, S$_{\alpha}$ $\approx$7.2 MeV) at beam energies of E$_{beam}$ $\geq$10 MeV/A. In contrast, the recent spectroscopic efforts typically use beams of more weakly bound nuclei such as ^{7}Li (^{7}Li$\rightarrow$ α+t, S$_{\alpha}$ $\approx$2.5 MeV) and ^{9}Be (^{9}Be$\rightarrow$ α+^{5}He, S$_{\alpha}$ $\approx$2.5 MeV) at energies a few MeV above the Coulomb barrier. There is also active research interest in the break–up and fusion processes of weakly bound stable nuclei at near–barrier and sub–barrier energies [18–21] as a precursor to similar studies using radioactive–ion beams.

If such reactions are to be fully exploited for spectroscopy then a more quantitative understanding of the mechanism of energy and angular momentum transfer is needed. For instance, it is generally recognized that cross-sections for specific nuclei formed via channels involving charged–particle emission are generally much higher (by one to two orders of magnitude) than the predictions of standard fusion–evaporation models. However, there are few quantitative measurements or calculations, especially for the reactions of interest to spectroscopists. In this paper we report on our efforts to fill this gap in our understanding.

We have used the binary transfer model of Wilczyński et al. [16,17] to calculate the cross–sections of different transfer components in ^{7}Li-induced binary reactions. We then use these results as input to a standard evaporation model [22]. By assuming that the energy of the beam is shared between the captured and emitted fragments in proportion to their mass, and accounting for the ground–state Q–values of each reaction channel, we are able to predict cross–sections for specific final nuclei. The predictions are compared to experimental results for two different reactions: ^{7}Li+^{160}Gd and ^{7}Li+^{184}W. The former set of data was taken from a recent publication by Jungclaus *et al.* [10], while the latter came from the first experiment performed using the new LIBERACE (Livermore Berkeley Array for Collaborative Experiments) Ge–array in combination with the STARS (Silicon Telescope Array for Reaction Studies) particle–detector system [23] at the 88–Inch Cyclotron of the Lawrence Berkeley National Laboratory. We find good quantitative agreement between the calculations and experimental data.

First, we briefly describe the Wilczyński model and the method used to calculate the cross-sections for populating different channels. Second, we compare the calculations with the existing experimental information on the ^{7}Li+^{160}Gd [10] reaction. Third, we describe the experimental set-up for the ^{7}Li+^{184}W measurements and compare the results with our predictions. Finally, we discuss outstanding issues and propose ideas to address them.

II. THEORETICAL MODEL OF THE REACTION PROCESS

The Wilczyński model [16,17] treats all binary reactions (in this context 'binary' refers to a two–body interaction producing nuclei in excited final states, the decay of which can be ignored in the description of the reaction mechanism) involving transfer of one or more nucleons, up to and including complete fusion, in exactly the same way. It is known experimentally that for this class of reactions the cross–sections have an exponential dependence on the ground–state Q–value, Q_{gg} [24]. This was interpreted as a consequence of a partial statistical equilibrium achieved during the collision such that the probabilities of specific

final configurations are proportional to the final–state level densities [25]. Therefore, it was suggested that the probability, *p(i)*, of a given channel i, being one component of the many possible binary transfer processes, is proportional to an exponential factor such that:

$$p(i) \propto exp\left(\frac{Q_{gg}(i) - Q_C(i)}{T}\right) \tag{1}$$

where T is an effective temperature treated as a free parameter and Q_C is the difference in the Coulomb interaction due to the transfer of charge. This term can be written as (in MeV):

$$Q_C = 1.442 q_C \left(Z_1^f Z_2^f - Z_1^i Z_2^i\right) \tag{2}$$

where Z_1^i, Z_2^i and Z_1^f, Z_2^f are the initial and final proton numbers in the dinuclear system before and after the binary reaction, respectively, and q_C is a free parameter in units of fm^{-1}.

The next assumption is based on a generalization of the concept of critical angular momentum for a reaction [26]. This states that the transfer of mass can only occur below a critical value of the angular momentum, l_{cr}, of relative motion of the captured fragment and absorbing nucleus. Above this value, there is no potential barrier against fission and the compound system cannot survive. For each channel, involving the capture of a particular fragment from the projectile, the limiting angular momentum, l_{lim}, is approximated by:

$$l_{lim} \simeq \frac{A_{proj}}{A_{cap}} l_{cr} \tag{3}$$

where A_{proj} and A_{cap} are the mass numbers of the projectile and captured fragments, respectively. The critical angular momentum, derived from equilibrium of forces, can be calculated using the formula [26]:

$$\left(l_{cr} + \frac{1}{2}\right)^2 = 0.02392\mu \left(C_c + C_t\right)^2 \left(4\pi\gamma \frac{C_c C_t}{C_c + C_t} - \frac{1.442 Z_c Z_t}{\left(C_c + C_t\right)^2}\right) \tag{4}$$

where μ is the reduced mass of the system comprising the captured fragment plus target and γ is a surface tension coefficient (typically, $\gamma \approx 0.95$). C_c and C_t are the half–density radii

of the captured fragment and target nucleus, respectively, which can be calculated from the equivalent sharp radii, R, using a standard parameterization [26–28]:

$$C = R\left(1 - \frac{b^2}{R^2}\right) \tag{5}$$

with b=1 fm.

The transmission coefficient for a given angular momentum, l, and specific reaction channel, i, may be written as:

$$T_l(i) = \left(1 + exp\left[\frac{l - l_{lim}(i)}{\Delta_l}\right]\right)^{-1} \tag{6}$$

Δ_l is a free parameter which smooths the cut-off in angular momentum. The absolute reaction cross–section for each channel is then written as:

$$\sigma\left(i\right) = \frac{\pi\hbar^2}{2\mu E}\sum_{l=0}^{l_{max}}\left(2l+1\right)\frac{T_l\left(i\right)p\left(i\right)}{\sum_j T_l\left(j\right)p\left(j\right)} \tag{7}$$

The sum over the partial waves in equation (7) is limited by the largest angular momentum for which any reaction can take place, l_{max}. We use the value calculated for a grazing collision between the beam and target nuclei as described in [26].

Using this prescription, we are then able to calculate the cross–sections for channels formed in a given reaction. This method was used to succesfully reproduce experimental results on transfer channels created in the reactions ^{12}C+^{160}Gd (E_{beam} in the range 7.5 – 16.7 MeV/A) and ^{14}N+^{159}Tb (E_{beam} = 10 MeV/A) [16,17]. We reproduced those results and then calculated cross–sections for channels formed in ^{7}Li–induced reactions over a wide range of energies. Reaction channels involving the emission of n, ^{1,2,3}H, ^{3,4,5,6}He, and ^{6,7}Li were included in equation (7). Fig. 1 shows a typical set of channel cross–sections calculated for the ^{7}Li+^{184}W reaction for several beam energies. It is clear that there are sizeable cross–sections for many of the transfer channels over the full range of energy.

The next step is to calculate the cross–section of forming a particular residue after evaporation of nucleons from the excited heavy nucleus formed in the binary transfer reaction. This was done using a standard evaporation code [22]. We assume that the beam energy

is shared in proportion to the masses of the captured and emitted fragments. The energy involved in the breakup of the projectile is taken into account. The evaporation code can then be run for each of the different reaction channels corresponding to a given energy of the beam. The calculation yields the fraction of the cross–section, *f(i)*, of a given binary reaction channel, *i*, that ends up in a specific residual nucleus. Finally, the total cross-section of formation of a residual nucleus, σ_{res}, at a given beam energy can be found by summing all the components for that residue formed in all the different transfer channels:

$$\sigma_{res} = \sum_i f(i)\sigma(i) \tag{8}$$

Fig. 2 shows the calculated cross-sections for various residual nuclei formed in the ^{7}Li+^{184}W reaction over a range of beam energies.

III. COMPARISON TO EXPERIMENTAL DATA ON ^{7}LI+^{160}GD

To test the model we used the results reported by Jungclaus *et al.* on the ^{7}Li+^{160}Gd reaction [10]. This reaction was successfully used to populate new high–angular–momentum states in several neutron–rich Dy nuclei [10,11]. As part of the study an excitation function was performed and relative cross–sections for populating the different Dy isotopes were estimated from the measured γ–ray flux into the ground–states of the different Dy isotopes. These were converted into absolute cross–sections by measuring the total X–ray flux. Significant systematic errors can occur with such measurements if the decay schemes involved are complex and especially if there are isomeric states present. This is true for the Ho and Tm nuclei populated in the reaction but the Dy nuclei that were studied have well–established low–angular–momentum level schemes allowing reasonable estimates of the absolute cross–sections to be made.

Fig. 3 shows the experimental results (with a nominal 20% error bar [10]) for the total cross–section going into any Dy nucleus as a function of beam energy. For comparison is shown the prediction from a standard fusion–evaporation model. Such a model significantly

underestimates the population of the Dy nuclei. A calculation using the Wilczyński model, as described above, is also shown and the agreement is very good. In this latter picture the Dy nuclei are formed from the massive transfer of 'He'–like fragments (^{4,5,6}He) from ^{7}Li to the ^{160}Gd nucleus.

Taking into account the evaporation of nucleons (mainly neutrons) from the excited heavy nucleus, as described in the previous section, we can calculate the cross–sections for forming particular residual Dy nuclei. A comparison with the experimental data is given in Fig. 4. The absolute cross-sections for the strongest residues are reproduced to within a factor of two. ^{162}Dy is populated with a very large cross–section over a wide range of beam energies (40–60 MeV). We see that the population of ^{161}Dy gradually increases and starts to dominate at the highest experimental energies (>60 MeV). This feature of one or two residues having the largest cross–sections over a wide range of beam energy is a consequence of the energy sharing between the captured and emitted fragments and the fact that the residues are formed in several of the different binary channels involving transfer of 'He'–like fragments at any given beam energy. Changing the beam energy by ≈10 MeV, which would shift the dominant neutron evaporation channel in a complete fusion reaction, will have less effect on the relative population of the residues formed in the transfer channels. This should be a general feature of these light–ion induced binary transfer reactions.

IV. EXPERIMENTAL INVESTIGATION OF THE ^{7}LI+^{184}W REACTION

We performed an experiment to test the model further. The ^{7}Li+^{184}W reaction was used at beam energies in the range 40–70 MeV. The beam, accelerated by the 88–Inch Cyclotron of the Lawrence Berkeley National Laboratory, was incident on a target comprising a 2.27 mg/cm^2 self–supporting foil of enriched ^{184}W.

Charged–particles were detected with the STARS (Silicon Telescope Array for Reaction Studies) Si ΔE–E telescope system which consisted of two annular silicon strip detectors with inner radius 11 mm and outer radius 59 mm. The detectors were electrically segmented

into 24 concentric rings on the front face and 8 wedge–shaped sectors on the back face. The ΔE detector was of $\approx$140 μm thickness while the E detector was $\approx$1000 μm in thickness. The detectors were placed at forward angles with respect to the beam direction. The configuration had a target–to–detector distance of $\approx$3 cm to the ΔE detector which was separated from the E detector by $\approx$1 cm. This gave an angular coverage from $\approx$20° to $\approx$55° with respect to the beam direction.

Gamma rays were detected with the new LIBERACE (Livermore Berkeley Array for Collaborative Experiments) Ge–detector array which consists of up to six Compton–suppressed clover detectors situated in the horizontal plane around the target chamber with two detectors each at $\pm$45° and two at 90°. The distance between the target and the front of each Ge detector was $\approx$17.25 cm.

In a first experiment, with only five of the six possible Ge detectors in place, data were collected at three different beam energies: 42, 49, and 55 MeV. For each run, the trigger for collecting an event was defined as either a coincidence between a charged particle and at least one Compton–suppressed gamma ray or detection of two or more Compton–suppressed gamma rays. Approximately 42×10^6, 43×10^6, and 120×10^6 events were collected at 42, 49, and 55 MeV, respectively. A second experiment, at beam energies of 40 and 70 MeV, was also performed. For this latter experiment, the full complement of six Ge detectors were in place. The STARS detectors were removed in order to maximize collection of γ–ray data. An event was defined as a coincidence of two or more Compton–suppressed gamma rays. Totals of approximately 300×10^6 and 110×10^6 events were recorded at 40 and 70 MeV, respectively.

The γ–ray data were sorted into a variety of E_γ–E_γ matrices and particle–gated spectra. To create ΔE–E matrices for particle identification, a 'ray–tracing' requirement was imposed such that, for particles detected in a specific ring of the ΔE detector, the associated signal from the E detector must have come from any of the three neighboring rings that lie closest to the line–of–sight defined by the target and ΔE ring. This greatly reduces background in the ΔE–E matrices and allows clear identification of emitted α's, protons, deuterons, and

tritons. A typical ΔE–E plot is shown in Fig 5.

It was not possible to accurately determine the relative cross–sections of the different residual nuclei from the γ–ray flux to the ground–states. The decay schemes of the odd–A Ir, Os, and Re nuclei are poorly known, complex, and involve many long–lived isomers. The situation is even worse for the odd–odd Re isotopes. However, based on the gamma–ray data we are able to make some qualitative observations. Moreover, the particle information allows a more quantitative comparison with our predictions of the relative probabilities of the emission of the different types of charged particles at the different beam energies (see Fig. 1). First we turn to a qualitative discussion of the γ–ray data.

Fig. 6 shows part of the total projection of the E_γ–E_γ matrix taken at E_{beam}=40 MeV. We clearly see that ^{187}Ir, formed primarily from the complete fusion of the ^{7}Li beam followed by evaporation of four neutrons, is the strongest channel. This is expected from the calculations presented in Fig. 2a. One of the next strongest channels is ^{185}Re which is formed in transfer channels involving the capture of 'H'–like fragments followed by evaporation of neutrons from the compound nucleus. Again, this is in good qualitative agreement with the calculation (see Fig. 2b). As yet, we have not been able to clearly identify ^{184}Re, which is predicted to be the next most intense Re nucleus. This is not surprising since it is expected to be much more weakly populated (by about a factor of ten) than ^{185}Re and the low–lying level scheme is very poorly known with only three γ–rays assigned beneath an isomeric state. For the Os nuclei, formed in transfer channels involving the capture of 'He'–like fragments, we clearly see ^{186}Os. We are not able to identify states from ^{187}Os, which is predicted to be the strongest Os residue (see Fig. 2c). However, careful analysis indicates that we see transitions in ^{188}Os. This is illustrated by the coincidence spectrum presented in Fig. 7.

It is difficult to think of a scenario in which ^{186}Os and ^{188}Os are both created simultaneously in transfer channels while ^{187}Os is not. We believe that the explanation is likely to lie with the angular momentum involved in the transfer process. It is seen in Fig. 7 that the intensity of the ground–state sequence in ^{188}Os falls rapidly and we are only able to identify states up to the 8^+ level. In ^{187}Os, an $11/2^+$ state is already yrast at 257 keV (the

ground–state is $1/2^-$) and if we are only weakly populating levels at higher angular momentum, as is the case in ^{188}Os, then there will only be a few transitions in ^{187}Os, mainly at low energy ($\leq$100 keV), which are difficult to identify. The problem is compounded by the fact that the intensity in an odd–A nucleus in this region is likely to be split among several strongly coupled bands involving low–energy transitions. The angular momentum transfer in these binary transfer channels is an issue we would like to address in future studies aimed at nuclei better suited to the investigation (for example, nuclei in the rare–earth region with well known rotational decay schemes).

Fig. 8 shows part of the total projection of the E_γ–E_γ matrix taken at E_{beam}=70 MeV. The strongest xn–channel appears to be ^{185}Ir while transitions in both the neighboring odd–odd Ir isotopes are also seen. This agrees with the predictions shown in Fig. 2a. For the Re isotopes the strongest channel is ^{183}Re. ^{184}Re should also be strongly populated (see Fig. 2b) but, as discussed above, difficult to identify. For the Os nuclei, yrast transitions in ^{184}Os and ^{186}Os are readily identified. We also see transitions in ^{185}Os, which is predicted (see Fig. 2c) to be the strongest Os residue at this energy, but the intensity is fragmented among several different sequences.

Similar examination of the γ–ray data at all the different beam energies shows a very good qualitative agreement with the calculations shown in Fig. 2. This is in itself a very important step forward. These results illustrate the potential of predicting the relative population of the transfer channels which will help the optimization of spectroscopy experiments.

Turning to the particle information we are able to make more quantitative comparisons with the calculations. Fig. 9 shows, for each ring in the ΔE Si detector, the ratio of the number of α–particles to the number of tritons, I(α/t), and the ratio of the number of tritons to the number of deuterons, I(t/d), for the reaction at E_{beam}=55 MeV. These ratios were estimated by integrating the counts in a two–dimensional region of a given particle–identifcation ΔE–E plot such as that shown in Fig. 5. A significant fraction of the protons have energy sufficient to punch through the thicker E Si detector and fall below the detection threshold. This effect was much less for the deuterons and tritons. We did not use the proton

information to construct ratios to compare with the calculations.

From Fig. 9 it is seen that there is no strong angular dependence on the deduced ratios. This indicates that, over the angular range covered by the STARS detectors, the different types of emitted particles have similar angular distributions. We find that at E_{beam}=55 MeV the average values for the particle ratios are I(α/t)= 3.83(14) and I(t/d)=1.10(4). The calculated values are I(α/t)=4.07 and I(t/d)=1.06. This agreement is very good. Fig. 10 shows these same ratios measured at beam energies of 42, 49, and 55 MeV in comparison to the calculated values. In this range of energies we find that the measured ratios are approximately constant with I(α/t)$\approx$4 and I(t/d)$\approx$1. The calculation is in good agreement.

Overall, we have good quantitative agreement between the measured numbers of particles and the Wilczyński binary transfer model. In addition, after accounting for nucleon evaporation, we have a good qualitative understanding of the γ–rays seen from the different residual nuclei at each energy.

V. SUMMARY AND CONCLUSION

We have used the model of Wilczyński et al. [16,17] to calculate the cross–sections of different transfer components in ^{7}Li-induced binary reactions. Using these results as input to a standard evaporation model [22], we have predicted cross–sections for specific final nuclei. The predictions were compared to experimental results for two different reactions: ^{7}Li+^{160}Gd and ^{7}Li+^{184}W. The former set of data was from a recent publication by Jungclaus *et al.* [10], while the latter came from the first experiment performed using the new LIBERACE–plus–STARS detector systems at the 88–Inch Cyclotron of the Lawrence Berkeley National Laboratory. In the case of the ^{7}Li+^{160}Gd reaction, we were able to make a quantitative comparison between the experimental and calculated cross–sections for final residual Dy nuclei formed in transfer channels involving the capture of 'He'–like fragments. For the ^{7}Li+^{184}W reaction we made a qualitative comparison with the calculation for different final residues and also a quantitative comparison with the relative yields of emitted charged

particles. In all cases the agreement between measurement and calculation is good.

An outstanding issue is to investigate the angular momentum of final products formed in these binary transfer reactions. Some early efforts were made along this line [15,17] but the reactions involved beams and energies that would be of little interest to spectroscopists. It would also be interesting to investigate reactions involving other weakly bound stable beams, such as ^{9}Be and ^{11}B. Experiments with these beams indicate that it is possible to populate states with significantly higher angular momentum than can be reached with ^{7}Li–induced reactions [1]. Such properties need to be quantified if the reaction process is to be fully exploited. In this paper, we have made an attempt to address some of the issues associated with using binary transfer reactions for γ–ray spectroscopy. These reactions should be very useful for investigating neutron–rich heavy nuclei. When radioactive beams of neutron–rich light nuclei, in the appropriate energy range (5–10 MeV/A), become available such reactions may allow us to reach nuclei with even larger neutron excess.

ACKNOWLEDGMENTS

We would like to thank the operations staff of the 88–Inch Cyclotron. Support for LBNL was provided by the U.S. DoE under Contract Number DE–AC03–76SF00098. Part of this work was performed under the auspices of the U.S. Department of Energy by the University of California, Lawrence Livermore National Laboratory under Contract No. W–7405–ENG–48.

REFERENCES

[1] G.D. Dracoulis, A.P. Byrne, T.Kibédi, T.R. McGoram, S.M. Mullins, J. Phys. G 23 1191 (1997).

[2] G.D. Dracoulis, F.G. Kondev, A.P. Byrne, T. Kibédi, S. Bayer, P.M. Davidson, P.M. Walker, C. Purry, C.J. Pearson, Phys. Rev. C 53 1205 (1996).

[3] G.D. Dracoulis, S.M. Mullins, A.P. Byrne, F.G. Kondev, T.Kibédi, S. Bayer, G.J. Lane, T.R. McGoram, P.M. Davidson, Phys. Rev. C 58 1444 (1998).

[4] G.D. Dracoulis, A.P. Byrne, S.M. Mullins, T. Kibédi, F.G. Kondev, P.M. Davidson, Phys. Rev. C 58 1837 (1998).

[5] S.M. Mullins, A.P. Byrne, G.D. Dracoulis, T.R. McGoram, W.A. Seale, Phys. Rev. C 58 831 (1998).

[6] S.M. Mullins, G.D. Dracoulis, A.P. Byrne, T.R. McGoram, S. Bayer, R.A. Bark, R.T. Newman, W.A. Seale, F.G. Kondev, Phys. Rev. C 61 044315 (2000).

[7] T.R. McGoram, G.D. Dracoulis, T. Kibédi, A.P. Byrne, R.A. Bark, A.M. Baxter, S.M. Mullins, Phys. Rev. C 62 031303 (2000).

[8] A. Görgen, H. Hübel, D. Ward, S. Chmel, R.M. Clark, M. Cromaz, R.M. Diamond, P. Fallon, K. Hauschild, G.J. Lane, I.Y. Lee, A.O.Macchiavelli, K. Vetter, Eur. Phys. J. A 6 141 (1999).

[9] G.J. Lane, G.D. Dracoulis, A.P. Byrne, A.R. Poletti, T.R.McGoram, Phys. Rev. C 60 067301 (1999).

[10] A. Jungclaus, B. Binder, A. Dietrich, T. Hartlein, H. Bauer, Ch. Gund, D. Panegrau, D. Schwalm, J.L. Egido, Y. Sun, D. Bazzacco, G. de Angelis, E. Farnea, A. Gadea, S. Lunardi, D.R. Napoli, C. Rossi–Alvarez, C. Ur, G.B. Hagemann, Phys. Rev. C 66 014312 (2002).

[11] A. Jungclaus, B. Binder, A. Dietrich, T. Hartlein, H. Bauer, Ch. Gund, D. Panegrau, D. Schwalm, D. Bazzacco, E. Farnea, S. Lunardi, C. Rossi–Alvarez, C. Ur, G. de Angelis, A. Gadea, D.R. Napoli, X.R. Zhou, Y. Sun, Phys. Rev. C 67 034302 (2003).

[12] A. Jungclaus, A. Algora, M. Axiotis, M.J.G. Borge, M.A. Fernandez, A. Gadea, E. Galindo, M. Hausmann, S. Lenzi, T. Martinez, D.R. Napoli, I. Piqueras, R. Schwenger, C. Ur, Eur. Phys. J. A 20 55 (2004).

[13] T. Inamura, M. Ishihara, T. Fukuda, T. Shimoda, H. Hiruta, Phys. Lett. B 68 51 (1977).

[14] K. Siwek-Wilczyńska, E.H. du Marchie van Voorthuysen, J. van Popta, R.H. Siemssen, J. Wilczyński, Phys. Rev. Lett. 42 1599 (1979).

[15] K.A. Geoffroy, D.G. Sarantites, M.L. Halbert, D.C. Hensley, R.A. Dayras, J.H. Barker, Phys. Rev. Lett. 43 1303 (1979).

[16] J. Wilczyński, K. Siwek-Wilczyńska, J. van Driel, S. Gonggrip, D.C.J.M. Hageman, R.V.F. Janssens, J. Lukasiak, R.H. Siemssen, Phys. Rev. Lett. 45 606 (1980).

[17] J. Wilczyński, K. Siwek-Wilczyńska, J. van Driel, S. Gonggrip, D.C.J.M. Hageman, R.V.F. Janssens, J. Lukasiak, R.H. Siemssen, S.Y. van der Werf, Nucl. Phys. A 373 109 (1982).

[18] C. Signorini, Z.H. Liu, A. Yoshida, T. Fukuda, Z.C. Li, K.E.G. Lobner, L. Muller, Y.H. Pu, K. Rudolph, F. Soramel, C. Zotti, J.L. Sida, Eur. Phys. J. A 2 227 (1998).

[19] M. Dasgupta, D.J. Hinde, R.D. Butt, R.M. Anjos, A.C. Berriman, N. Carlin, P.R.S. Gomes, C.R. Morton, J.O. Newton, A. Szanto de Toledo, K. Hagino, Phys. Rev. Lett. 82 1395 (1999).

[20] V. Tripathi, A. Navin, K. Mahata, K. Ramachandran, A. Chatterjee, S. Kailas , Phys. Rev. Lett. 88 172701 (2002).

[21] M. Dasgupta, P.R.S. Gomes, D.J. Hinde, S.B. Moraes, R.M. Anjos, A.C. Berriman,

R.D. Butt, N. Carlin, J. Lubian, C.R. Morton, J.O. Newton, A. Szanto de Toledo, Phys. Rev. C 70 024606 (2004).

[22] A. Gavron, Phys. Rev. C 21 230 (1980).

[23] L.A. Bernstein, J.T. Burke, J.A. Church, L. Ahle, J.R. Cooper, R.D. Hoffman, J. Punyon, A. Schiller, E. Algin, C. Plettner, H. Ai, C.W. Beausang, R.F. Casten, R. Hughes, E. Ricard–McCutchan, D. Meyer, J.J. Ressler, J.A. Caggiano, N.V. Zamfir, H. Amro, A. Heinz, P. Fallon, M.A. McMahan, A.O. Macchiavelli, L.W. Phair, *Proceedings of International Conference on Nuclear Data for Science and Technology, Santa Fe, 2004*, AIP Conference Proceedings 769 890 (2005).

[24] A.G. Artukh, V.V. Avdeichikov, J. Ero, G.F. Gridnev, V.L. Mikheev, V.V. Volkov, J. Wilczyński, Nucl. Phys. A 160 511 (1971).

[25] J.P. Bondorf, F. Dickmann, D.H.E. Gross, P.J. Siemens, J. Phys. (Paris), Colloq. 32 C6 (1971).

[26] J. Wilczyński, Nucl. Phys. A 216 386 (1973).

[27] W.U. Schröder and J.R. Huizenga, Ann. Rev. Nucl. Sci. 27 465 (1977).

[28] W.D. Myers, Nucl. Phys. A 204 465 (1973).

FIGURES

FIG. 1. Excitation functions for the reaction channels formed in ^{7}Li+^{184}W collisions calculated with parameters T=4.5 MeV, q_C=0.06 fm^{-1}, and Δ_l=2 $\hbar$. Each channel is indicated by the emitted light fragment that remains after the transfer reaction.

FIG. 2. Calculated cross–sections of different residual nuclei formed in the ^{7}Li+^{184}W reaction at several different beam energies for: a) Ir nuclei formed in xn–type channels (relative to complete fusion of the beam and target); b) Re nuclei formed in αxn–type channels; c) Os nuclei formed in pxn–type channels.

FIG. 3. Cross–section as a function of beam energy for the sum of the charged–particle channels leading to any Dy nucleus in the ^{7}Li+^{160}Gd reaction. The dashed line is the calculation using a standard fusion–evaporation model. The solid line is the calculation using the Wilczyński model with parameters T=4.5 MeV, q_C=0.06 fm^{-1}, and Δ_l=2 $\hbar$.

FIG. 4. Cross–sections as functions of beam energy for the charged–particle channels leading to $^{160-164}$Dy in the ^{7}Li+^{160}Gd reaction. The left panel is the experimental data and the right panel the calculation. Solid (open) squares are for ^{160}Dy (^{161}Dy). Solid (open) circles are for ^{162}Dy (^{163}Dy). Solid triangles are for ^{164}Dy.

FIG. 5. A typical ray–traced ΔE–E matrix used for particle identification. The α's, protons, deuterons, and tritons are clearly separated.

FIG. 6. A section of the total projection of the E_γ–E_γ matrix taken at 40 MeV. Strong peaks belonging to various channels are indicated.

FIG. 7. A spectrum of gamma rays in ^{188}Os formed by requiring a coincidence with the 155 keV $2^+ \rightarrow 0^+$ transition. The angular–momentum assignment for each transition is indicated.

FIG. 8. A section of the total projection of the E_γ–E_γ matrix taken at 70 MeV. Strong peaks belonging to various channels are indicated.

FIG. 9. Plot of the ratio of the number of α–particles to the number of tritons, I(α/t), (solid circles) and the ratio of the number of tritons to the number of deuterons, I(t/d), (open circles) measured for the reaction ^{7}Li+^{184}W at E_{beam}=55 MeV as a function of the ID number of the ring in the ΔE Si detector. The solid lines are the calculated values.

FIG. 10. Plots of the ratio of the number of α–particles to the number of tritons, I(α/t), (solid circles) and the ratio of the number of tritons to the number of deuterons, I(t/d), (open circles) measured for the reaction ^{7}Li+^{184}W at different beam energies. The solid lines are the calculated values.

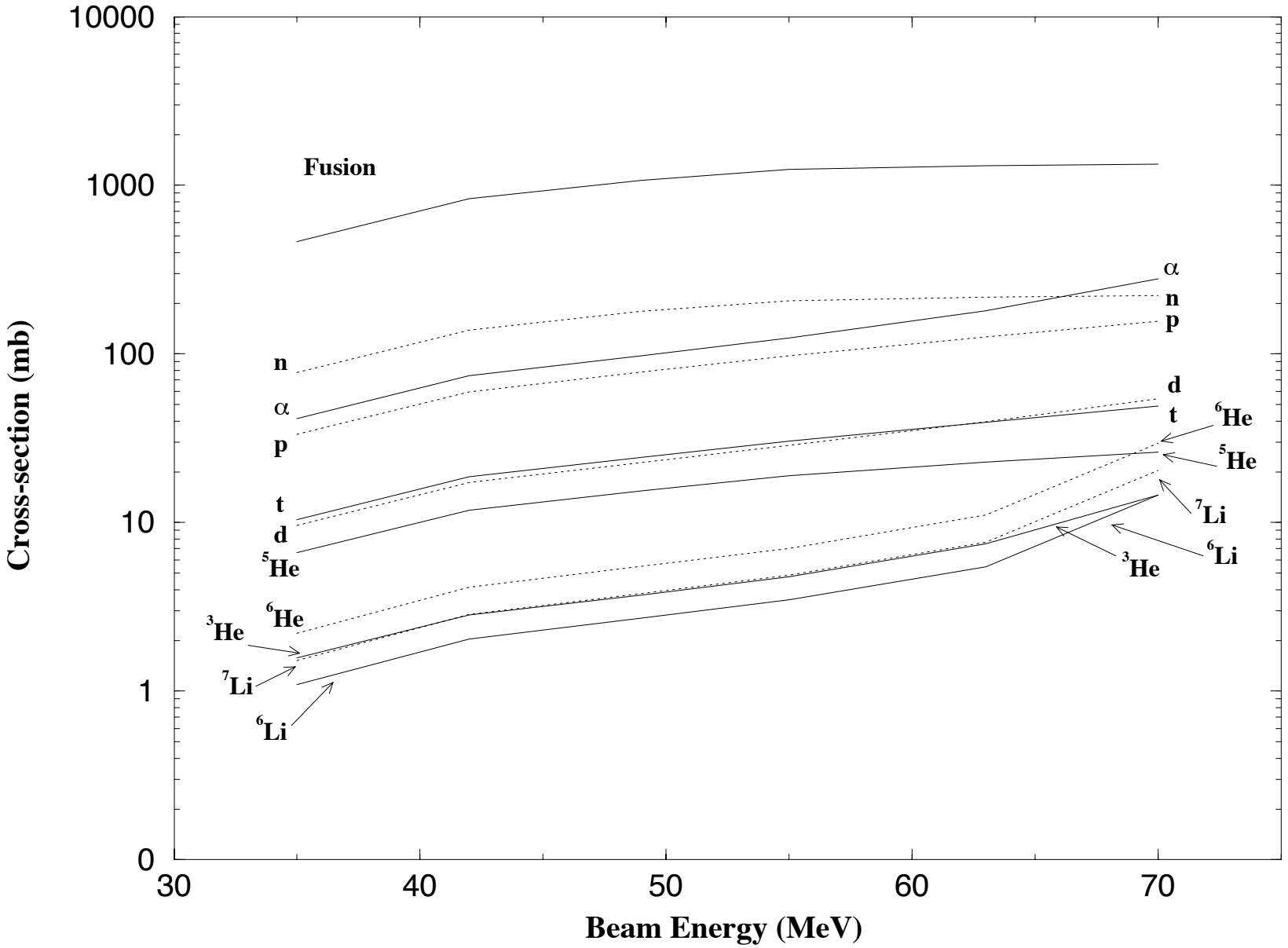
10000
1000
100
10
1
0
30
40
50
60
70
Cross-section (mb)
Beam Energy (MeV)
Fusion
α
n
p
d
t
6He
5He
7Li
6Li
3He

Fig.1, Clark

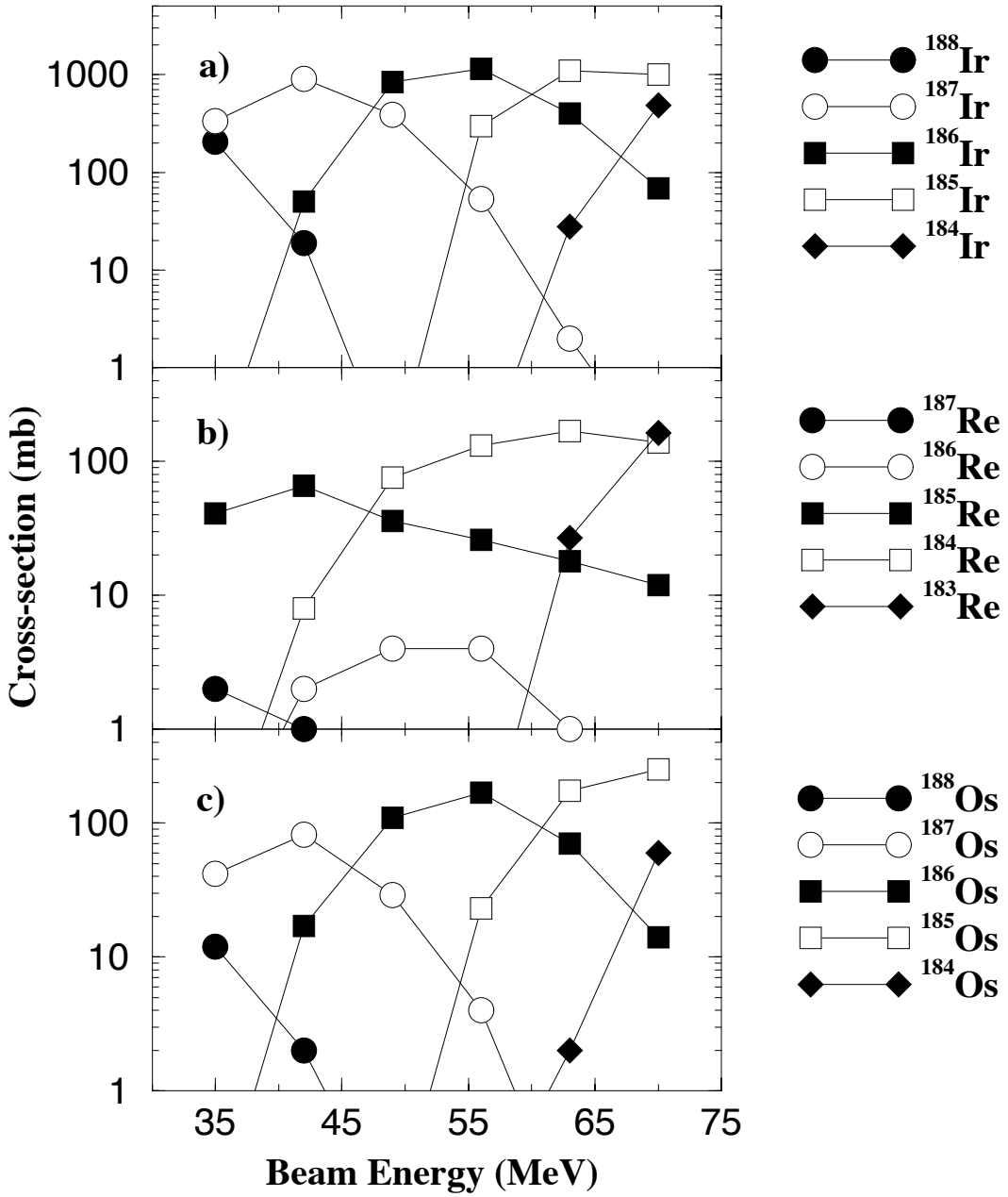
a)
b)
c)
1000
100
10
1
100
10
1
100
10
1
Cross-section (mb)
35
45
55
65
75
Beam Energy (MeV)
188Ir
187Ir
186Ir
185Ir
184Ir
187Re
186Re
185Re
184Re
183Re
188Os
187Os
186Os
185Os
184Os

Fig2, Clark

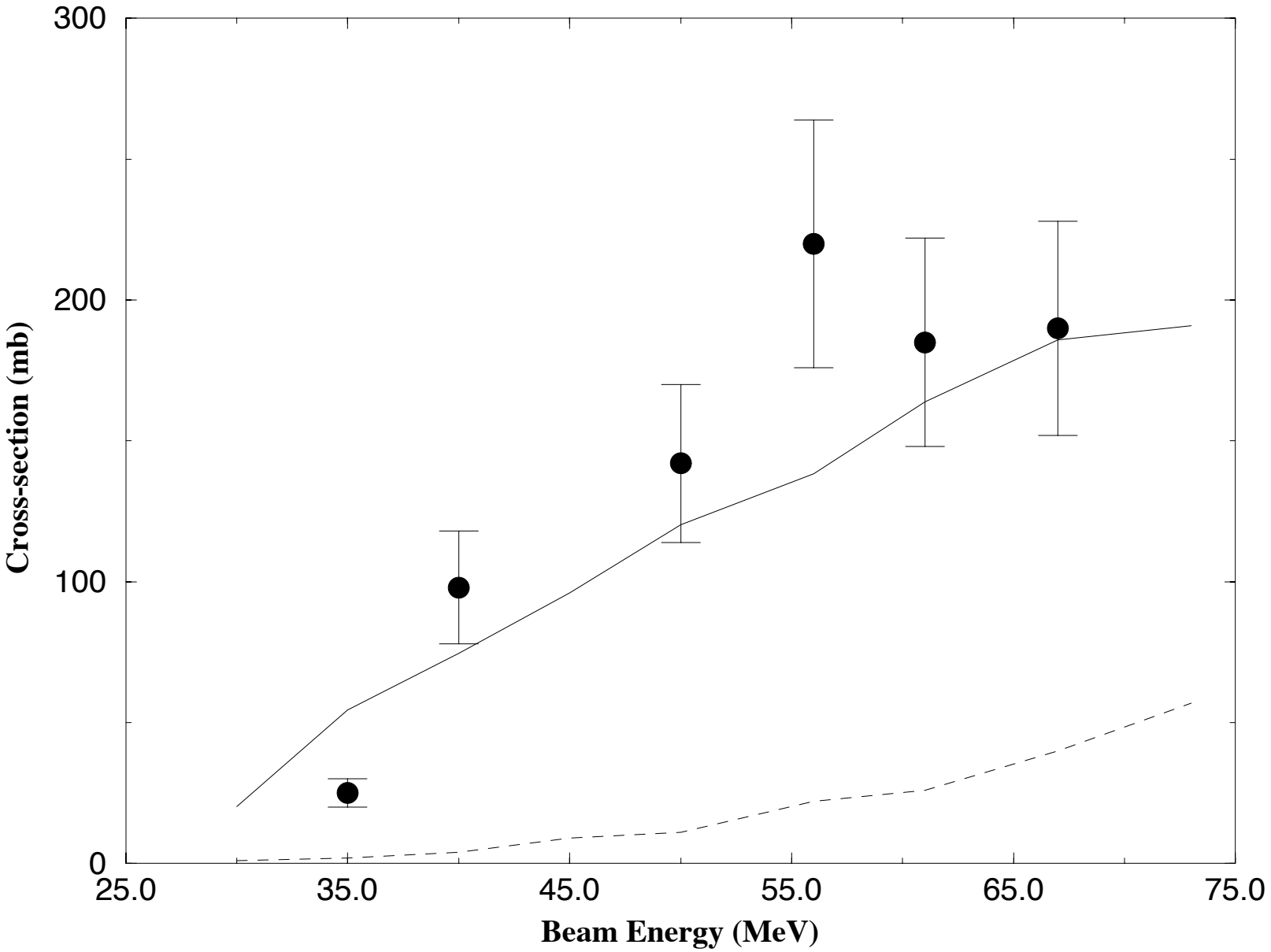
300
200
100
0
Cross-section (mb)
25.0
35.0
45.0
55.0
65.0
75.0
Beam Energy (MeV)

Fig.3, Clark

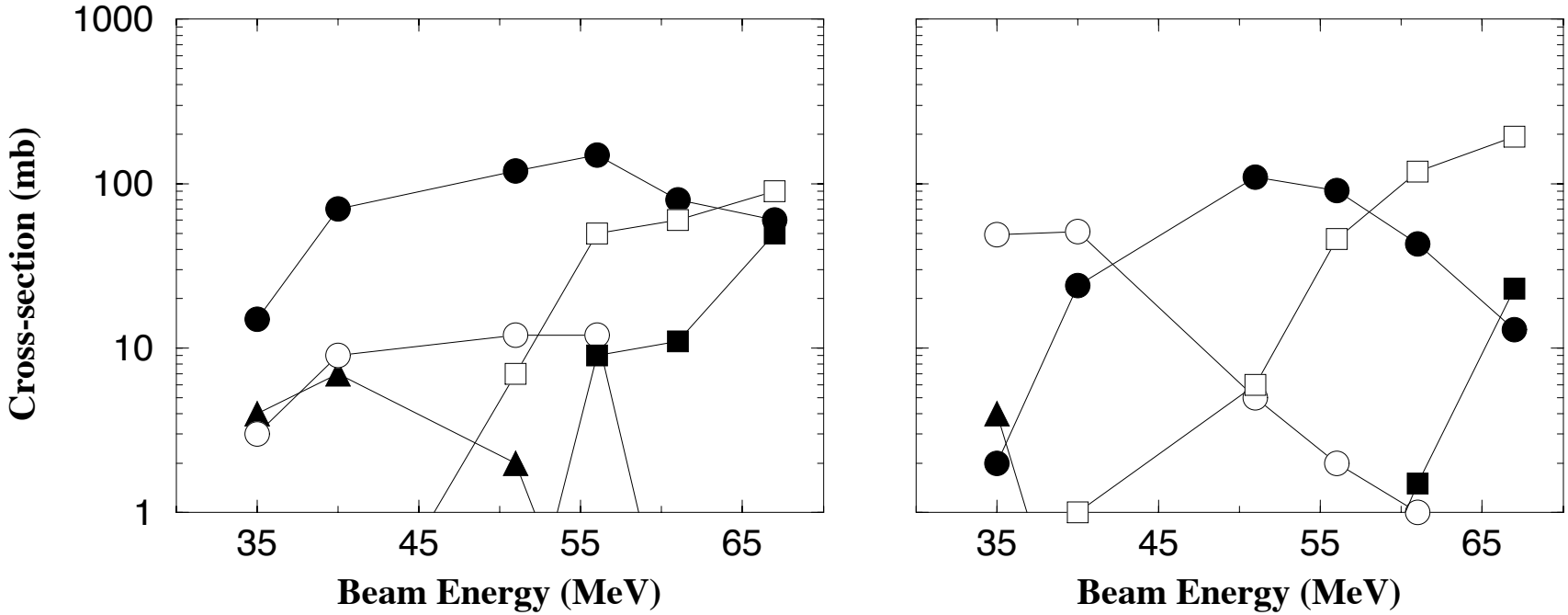
1000
100
10
1
Cross-section (mb)
35
45
55
65
Beam Energy (MeV)
35
45
55
65
Beam Energy (MeV)

Fig.4, Clark

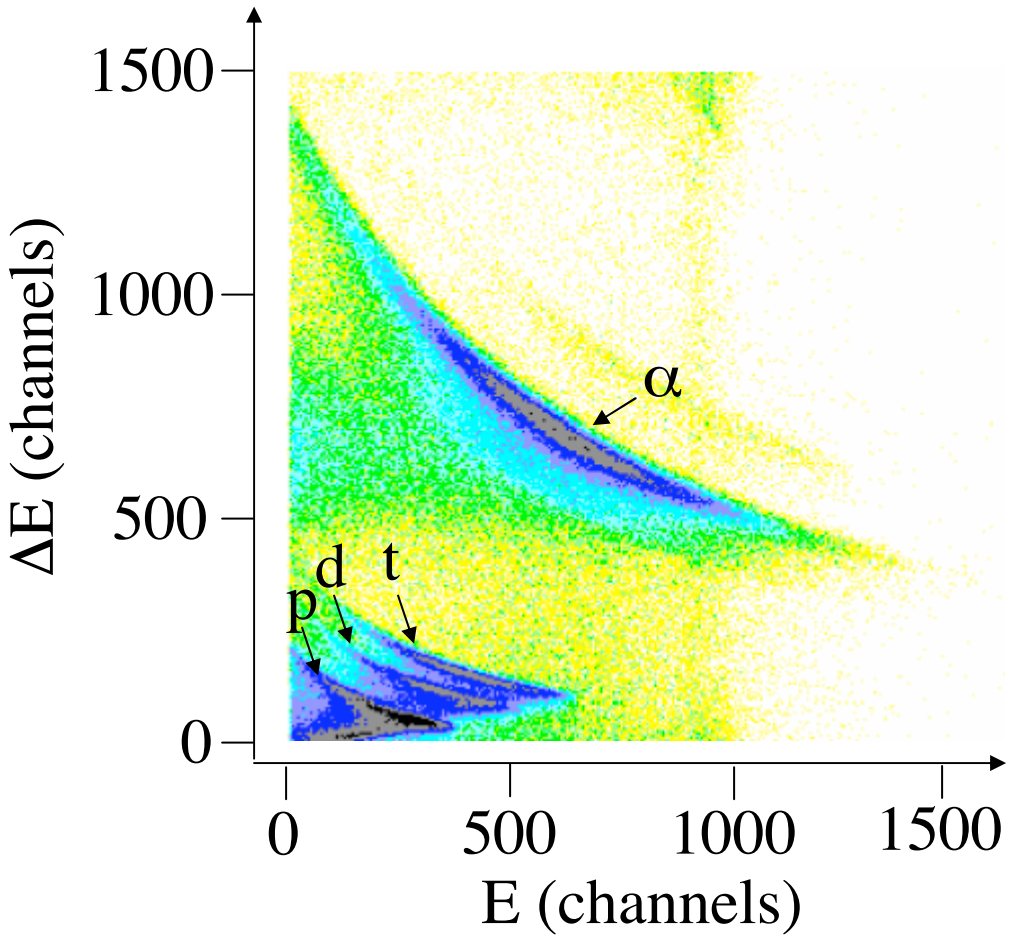

Fig.5, Clark

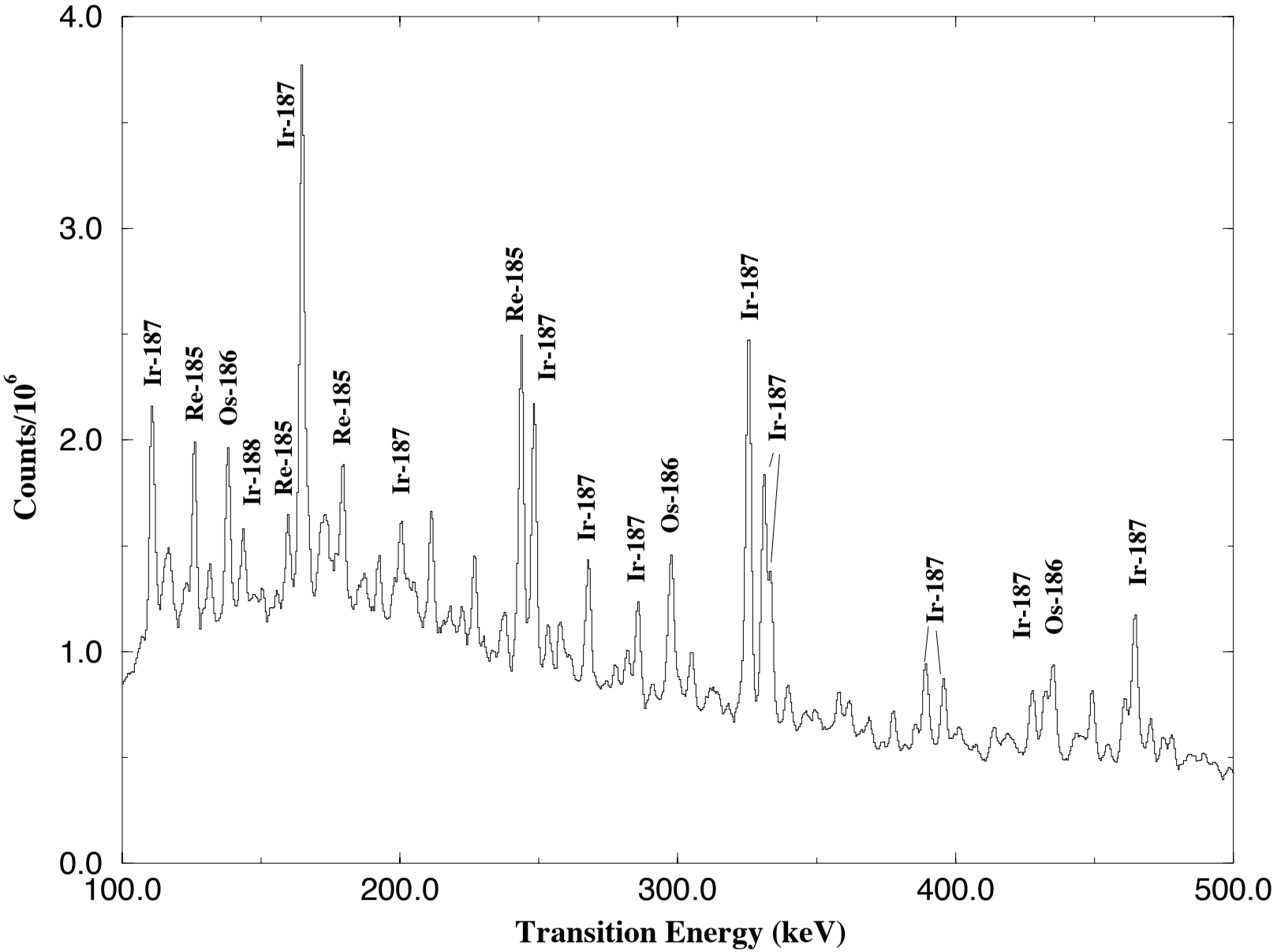
4.0
3.0
2.0
1.0
0.0
Counts/10^6
100.0
200.0
300.0
400.0
500.0
Transition Energy (keV)
Ir-187
Re-185
Os-186
Ir-188
Re-185
Ir-187
Re-185
Ir-187
Re-185
Ir-187
Ir-187
Os-186
Ir-187
Ir-187
Ir-187
Os-186
Ir-187

Fig.6, Clark

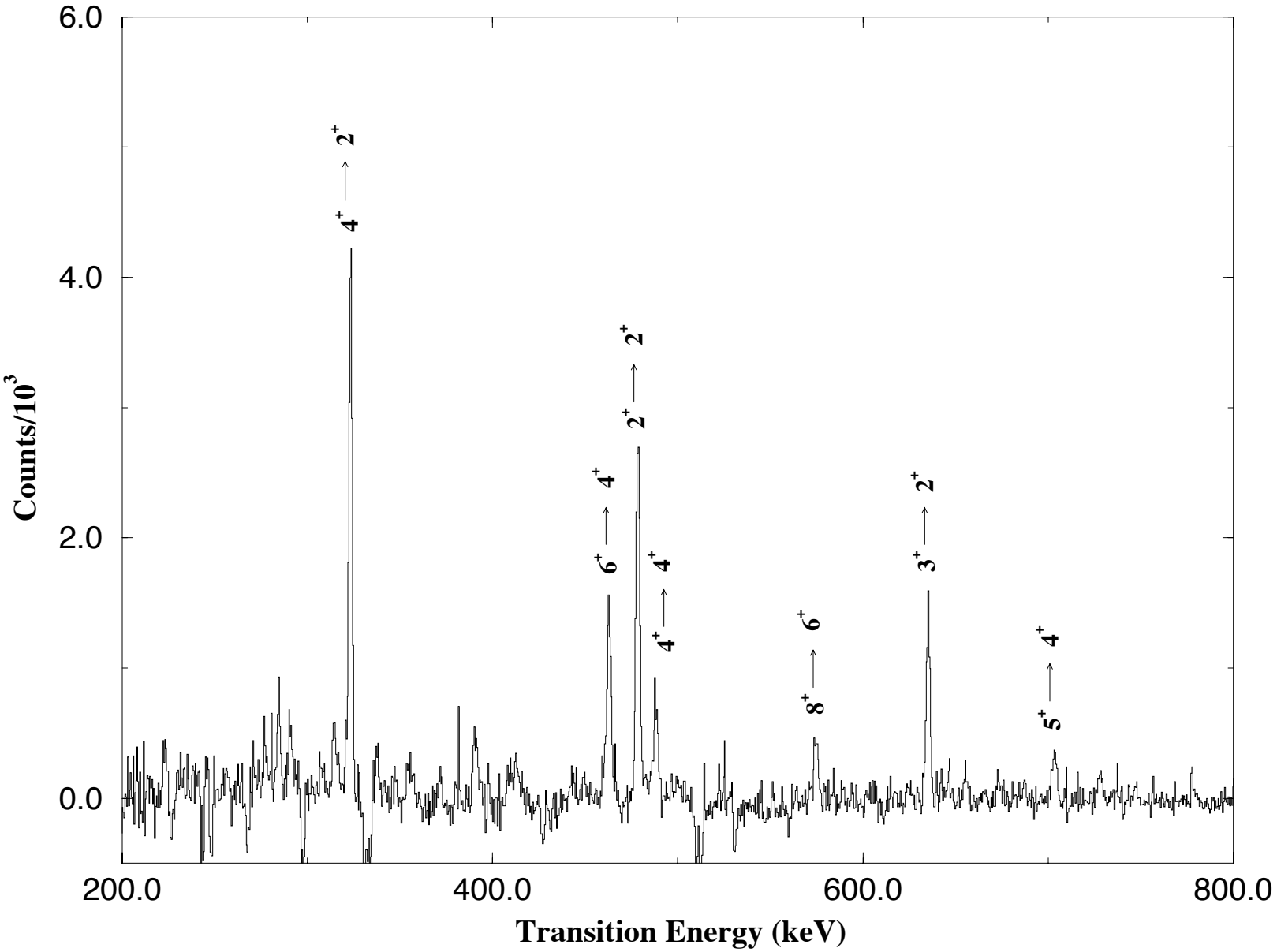
6.0
4.0
2.0
0.0
Counts/10^3
200.0
400.0
600.0
800.0
Transition Energy (keV)
4+ → 2+
6+ → 4+
2+ → 2+
4+ → 4+
8+ → 6+
3+ → 2+
5+ → 4+

Fig.7, Clark

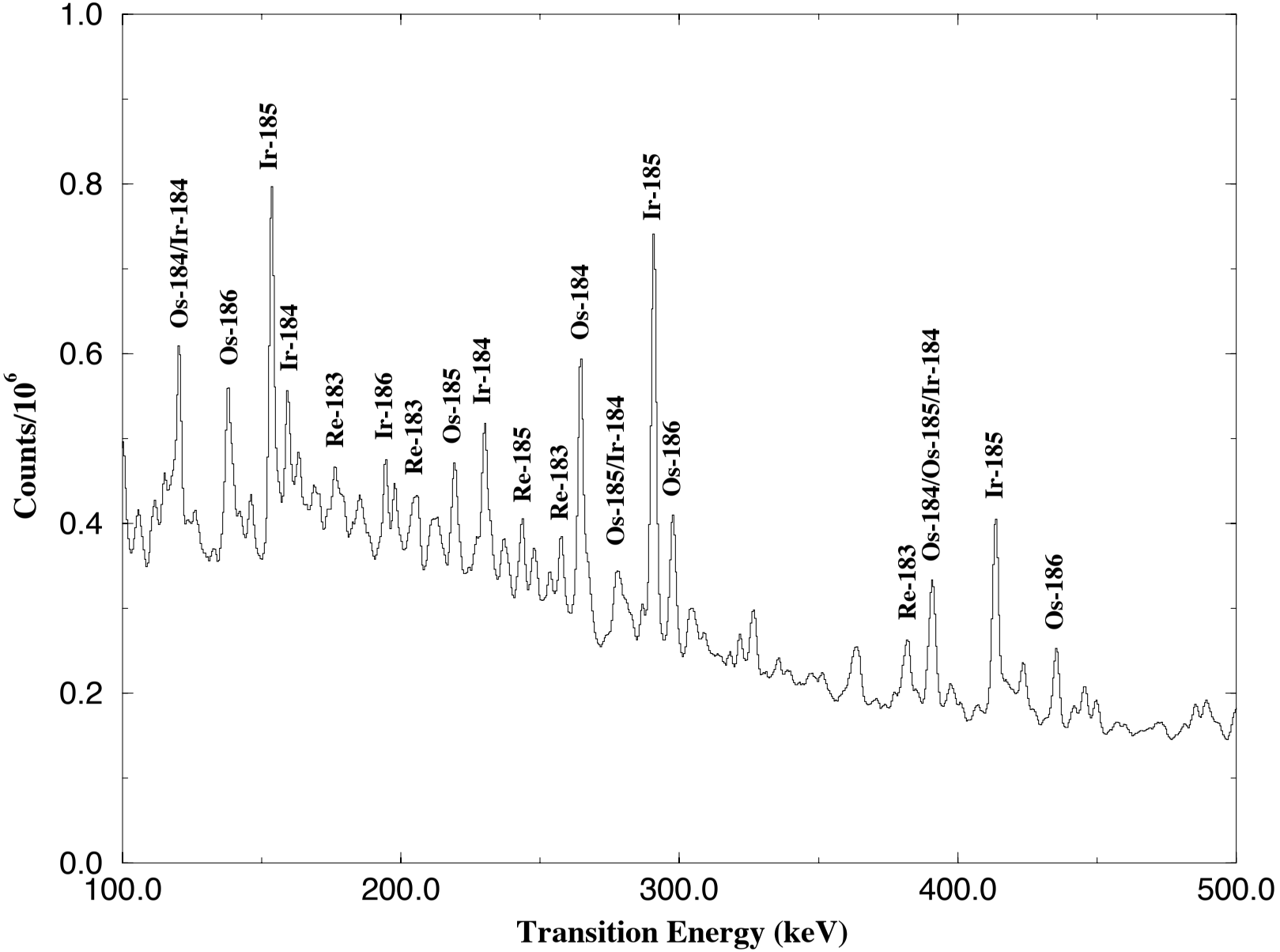
Counts/10^6
Transition Energy (keV)
1.0
0.8
0.6
0.4
0.2
0.0
100.0
200.0
300.0
400.0
500.0
Os-184/Ir-184
Os-186
Ir-185
Ir-184
Re-183
Ir-186
Re-183
Os-185
Ir-184
Re-185
Re-183
Os-184
Os-185/Ir-184
Ir-185
Os-186
Re-183
Os-184/Os-185/Ir-184
Ir-185
Os-186

Fig.8, Clark

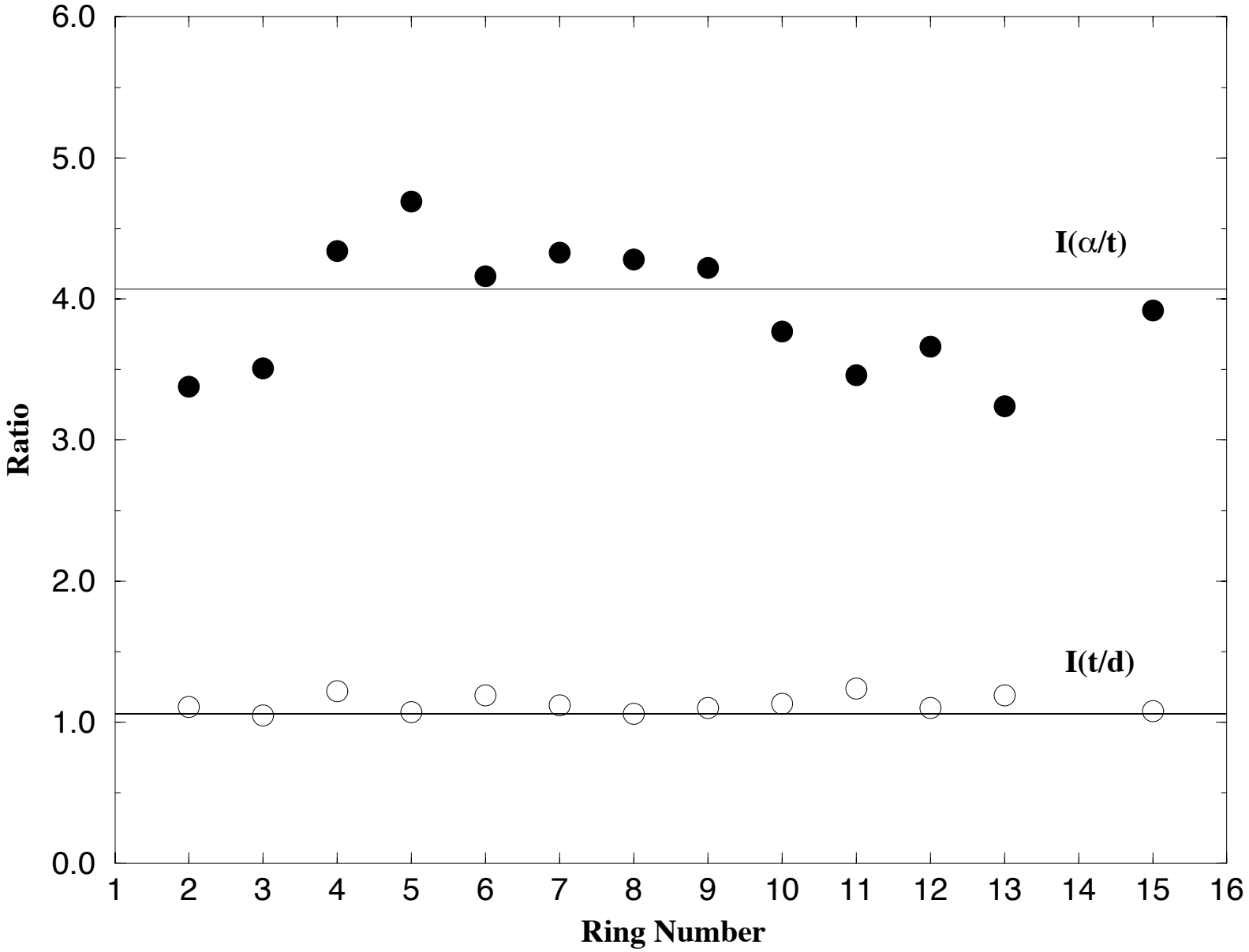
6.0
5.0
4.0
3.0
2.0
1.0
0.0
Ratio
I(α/t)
I(t/d)
1
2
3
4
5
6
7
8
9
10
11
12
13
14
15
16
Ring Number

Fig.9, Clark

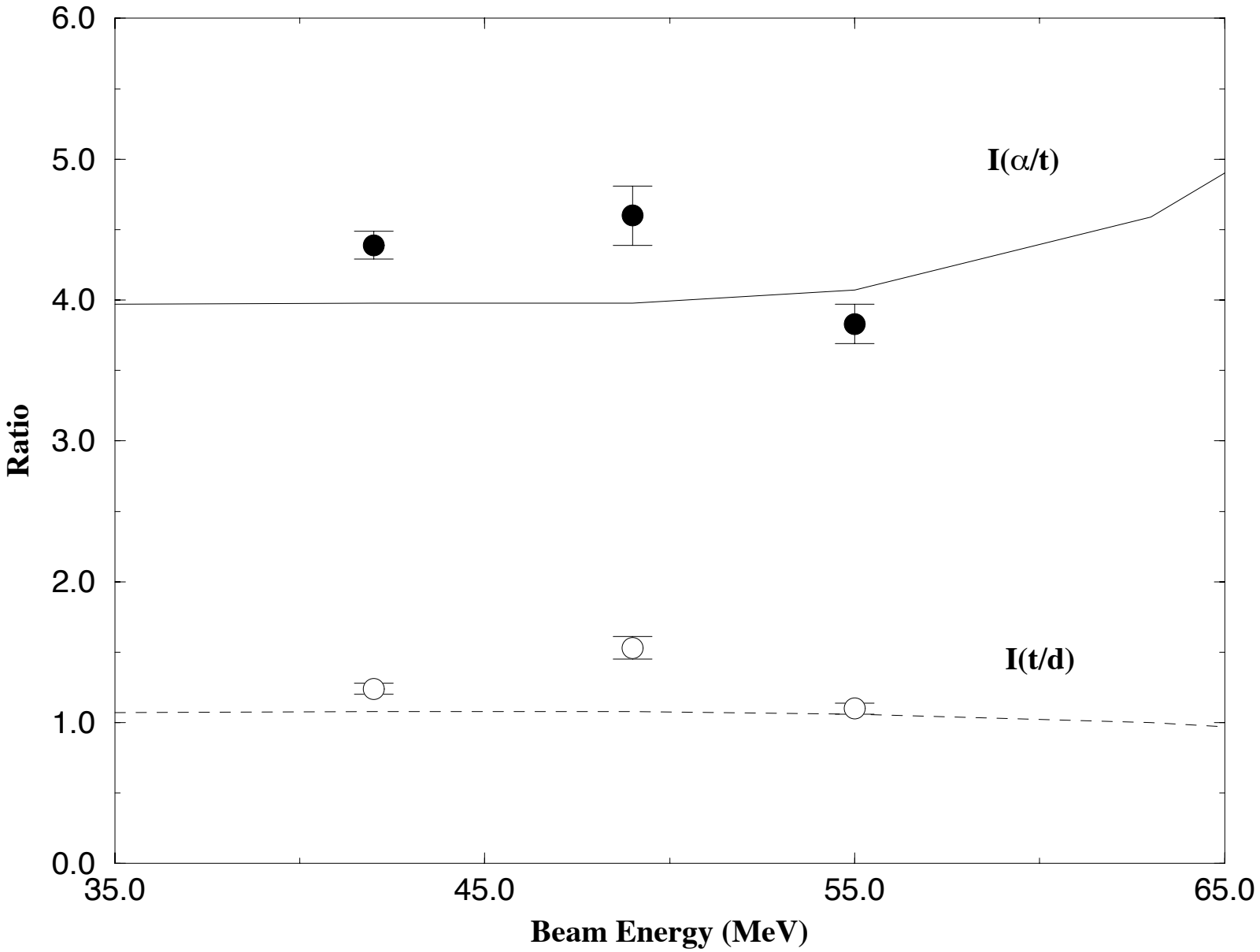
6.0
5.0
4.0
3.0
2.0
1.0
0.0
Ratio
I(α/t)
I(t/d)
35.0
45.0
55.0
65.0
Beam Energy (MeV)

Fig.10, Clark